

LIGHT-BY-LIGHT SCATTERING IN ULTRA-PERIPHERAL COLLISIONS IN THE FUTURE*

MARIOLA KLUSEK-GAWENDA

Institute of Nuclear Physics Polish Academy of Sciences, 31-342 Kraków, Poland

(Received May 8, 2019)

This work will be focussed on a study of photon-pair production that can be created through fermionic boxes, resonance scattering, VDM-Regge mechanism, two-gluon exchange and pionic background. Each of these processes dominates at different ranges of two-photon invariant masses. Presented nuclear cross sections are in good agreement with the recently measured ATLAS and CMS data. Predictions including ALICE and LHCb experimental cuts for the next run at the LHC will be shown.

DOI:10.5506/APhysPolB.50.1077

1. Introduction

Physics of the ultra-peripheral collisions (UPC) of heavy ions gives an opportunity to study electromagnetic processes. Due to the very strong electromagnetic field of colliding nuclei, reactions related to photon collisions can be studied. One can consider $\gamma\gamma$ fusion and photoproduction (Pomeron and/or Reggeon exchange) as a sub-process of heavy-ion UPC. Diphoton processes have long been studied at e^+e^- collider. This tool allows to test a QED theory and a lot of aspects of meson spectroscopy. Presented below results prove the theory that was proposed more than 80 years ago *i.a.* by Heisenberg and his students: Euler and Kockel [1, 2] or by Akhiezer, Landau and Pomeranchuk [3]. In e^+e^- collisions, the energies and couplings of photons to e^\pm are rather small so the corresponding $\gamma\gamma \rightarrow \gamma\gamma$ cross section is very small and, simultaneously, very difficult to measure. The light-by-light (LbL) scattering in ultra-peripheral collision is a relatively new issue.

2. $\gamma\gamma \rightarrow \gamma\gamma$ elementary cross section

The leading order of elementary cross section for $\gamma\gamma \rightarrow \gamma\gamma$ process is well-known and one can use the available to the general public Mathematica

* Presented at the Cracow Epiphany Conference on Advances in Heavy Ion Physics, Kraków, Poland, January 8–11 2019.

package: FormCalc [4]. Diagram (a) in Fig. 1 shows the so-called fermionic box (scattering via quarks and leptons is taken into account). The next diagram presents W^+W^- boson loop and this cross section is calculated within LoopTools [5]. Figure 1 (c) points out a diagram for non-perturbative mechanism of both photons fluctuations into light vector mesons (ρ, ω or ϕ) and their subsequent interaction. The soft VDM-Regge mechanism dominates at small transverse momentum of outgoing photons ($p_{t,\gamma} < 1$ GeV). The next diagram of Fig. 1 is of the same order in α_{em} as the previous one but has higher order in α_s . The two-gluon exchange mechanism is a three-loop mechanism [6]. The finite fermion masses, the full momentum structure in the loops and all helicity amplitudes are included. Quantitative comparison of the cross section as a function of outgoing photon transverse momentum shows that this elastic scattering could be studied experimentally in a future photon–photon collider. The two-gluon exchange mechanism starts to play important role at relatively large energies ($W_{\gamma\gamma} > 100$ GeV) and small values of $p_{t,\gamma}$ (from 1 to ≈ 5 GeV). Figure 1 (e) depicts production of resonances that decay into two-photon final state. Here, contributions from only pseudoscalar and scalar mesons are considered.

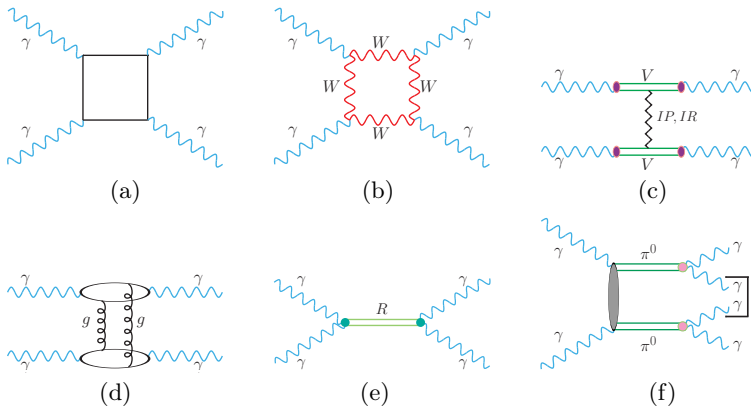


Fig.1. Light-by-light scattering mechanisms: with the fermionic loops (a), W -boson one-loop (b), the VDM-Regge (c), two-gluon exchange (d), resonances decay into $\gamma\gamma$ channel (e), and pionic background (f).

The role of mesons exchanges in the LbL scattering was comprehensively studied in Ref. [7]. There several pseudoscalar, scalar, tensor and 4-spin mesons were taken into account. The authors considered not only s -channel but also, for the first time, t - and u -channel meson exchange amplitudes corrected for off-shell effects including vertex form factors. Formally, the angular distribution for the s -channel resonances is used in calculating their contributions in the form of

$$\frac{d\sigma(\gamma\gamma \rightarrow R \rightarrow \gamma\gamma)}{dz} = \frac{1}{32\pi W_{\gamma\gamma}^2} \frac{1}{4} \sum_{\lambda_1, \lambda_2} |\mathcal{M}_{\gamma\gamma \rightarrow R \rightarrow \gamma\gamma}(\lambda_1, \lambda_2)|^2, \quad (1)$$

where $z = \cos\theta$ and θ denotes the polar angle between the beam direction and the outgoing particle in the c.m. frame, $W_{\gamma\gamma}$ — the invariant mass of the $\gamma\gamma$ system. The amplitude for the $\gamma\gamma$ production through the s -channel exchange of a pseudoscalar/scalar mesons takes the form of

$$\mathcal{M}(\lambda_1, \lambda_2) = \frac{\sqrt{64\pi^2 W_{\gamma\gamma}^2 \Gamma_R^2 \text{Br}^2(R \rightarrow \gamma\gamma)}}{\hat{s} - m_R^2 - im_R \Gamma_R} \times \frac{1}{\sqrt{2\pi}} \delta_{\lambda_1 - \lambda_2}. \quad (2)$$

In the present analysis, we take into account five mesons η , $\eta'(958)$, $\eta_c(1S)$, $\eta_c(2S)$, $\chi_{c0}(1P)$ whose masses m_R , total widths Γ_R or branching ratios $\text{Br}(R \rightarrow \gamma\gamma)$ are taken from PDG [8].

In addition, also a background from the $\gamma\gamma \rightarrow \pi^0(\rightarrow \gamma\gamma)\pi^0(\rightarrow \gamma\gamma)$ process is considered. A schematic diagram depicted in Fig. 1(f) shows the situation when as a result of gamma–gamma fusion, two neutral pions are created. These mesons decay into photons. We treat this process as a background only in the case when one photon from the first pion and one photon from the other pion are detected. If only two photons from different neutral pions are measured at a given experimental range of rapidities and transverse momenta, such an event could be wrongly identified as $\gamma\gamma \rightarrow \gamma\gamma$ scattering if no extra cuts are imposed to reduce or eliminate such a background. In Ref. [9], we constructed a multi-component model which described *e.g.* the Belle [10] and Crystal Ball [11] data for $\gamma\gamma \rightarrow \pi^0\pi^0$. In [9], both $\gamma\gamma \rightarrow \pi^+\pi^-$ and $\gamma\gamma \rightarrow \pi^0\pi^0$ reactions were considered within a multi-component model. There, for the first time, both the total cross section and angular distributions from the kinematical threshold ($W_{\gamma\gamma} = 2m_\pi$) up to the maximal experimentally available energy $W_{\gamma\gamma} \approx 6$ GeV were calculated. Simultaneously, the significance of nine resonances, $\gamma\gamma \rightarrow \pi^+\pi^- \rightarrow \rho^\pm \rightarrow \pi^0\pi^0$ continuum, the Brodsky–Lepage and handbag mechanisms in these processes was studied. The angular distribution for the $\gamma\gamma \rightarrow \pi^0\pi^0$ process in nuclear collisions can be calculated similarly as in Eq. (1). Then θ is the pion scattering angle. A detailed formalism and the description of these sub-processes can be found in [9].

3. Nuclear cross section

3.1. Theory

The nuclear cross section is calculated with the help of equivalent photon approximation (EPA) [12–14]. More precisely, we use equivalent photon

approximation in the impact parameter space. In this approach, the cross section is expressed through the 5-dimensional integral

$$\sigma_{A_1 A_2 \rightarrow A_1 A_2 X_1 X_2}(\sqrt{s_{A_1 A_2}}) = \int \sigma_{\gamma\gamma \rightarrow X_1 X_2}(W_{\gamma\gamma}) N(\omega_1, \mathbf{b}_1) N(\omega_2, \mathbf{b}_2) \times S_{\text{abs}}^2(\mathbf{b}) d^2b d\bar{b}_x d\bar{b}_y \frac{W_{\gamma\gamma}}{2} dW_{\gamma\gamma} dY_{X_1 X_2}, \quad (3)$$

where $X_1 X_2$ is a pair of produced particles. In the LbL scattering idea, it is just two-photon production. The EPA theory uses a concept of photon fluxes which depend on the energy of the photon (ω_i) and its impact parameter (\mathbf{b}_i). Here, we consider only ultra-peripheral collisions, that is, impact parameter (b) determining distance between centers of colliding nuclei is bigger than the sum of their radii. Vector \mathbf{b}_i is expressed through \bar{b}_x and \bar{b}_y components. The energy of produced particles is correlated with the energy of photons according to the dependence: $W_{\gamma\gamma} = 2\sqrt{\omega_1\omega_2}$ and rapidity of outgoing system is expressed through rapidity of singles particles: $Y_{X_1 X_2} = \frac{1}{2}(y_{X_1} + y_{X_2})$. Absorption factor $S_{\text{abs}}(\mathbf{b})$ assures UPC which means that nuclei pass each other being intact in the final state. We think that usage of EPA in the impact parameter space is more accurate in the context of UPC.

Our nuclear calculations are directed to LHC experiments. Each LHC detector has different acceptance. This acceptance very often is defined by some range of rapidity/pseudorapidity, transverse momentum of outgoing particles or transverse momentum of particle pair. Thus, we have to extend Eq. (3) by an additional dimension. This allows us to make a more accurate prediction or description of experimental data. We replace the total elementary cross section $\sigma_{\gamma\gamma \rightarrow X_1 X_2}$ by angular distribution. Then multi-dimensional distribution (grid) is prepared with the help of Monte Carlo simulation using the VEGAS algorithm [15].

The flux of photons $N(\omega, b)$, especially at small b , very strongly depends on the nuclear form factor. We prefer to use a realistic form factor in our calculation. Then nucleus is treated as an object with realistic charge distribution and two-parameter Fermi model is used to determination of nuclear density. Often a monopole and point-like form factor is used for the calculation. The comparison of results that include realistic and monopole form factor will be presented in the next subsection. The initial photon virtualities equal almost zero ($Q^2 \lesssim \frac{1}{R^2} \approx 800 \text{ MeV}^2$)¹, therefore, nuclear form factor kills large photon virtualities in UPC of heavy ions.

¹ R — nuclear radius $\approx 7 \text{ fm}$.

3.2. Predictions and comparison with experimental data

The LbL scattering was realized experimentally only recently by the ATLAS [16] and CMS [17] groups. For ions of charges Z_1, Z_2 , the cross section is enhanced by $Z_1^2 Z_2^2$ factor compared to proton–proton collisions, at least at low diphoton invariant masses equal to diphoton collision energies, where the initial photons are quasi real with extremely low virtualities. However, on the other hand, a significant part of cross section is cut off by the absorption factor (see Eq. (3)) which ensures ultra-peripheral character of the process. Nevertheless, UPC of heavy ion gave the first experimental verification of the theory proposed by Heisenberg *et al.* [1–3].

Our first paper [18] of the LbL scattering series presents an importance of fermion loop and non-perturbative mechanism of photons fluctuation into light vector mesons (VDM-Regge model) in ultra-peripheral lead–lead collisions. Quantitative comparison of these two mechanisms is presented in Fig. 2. One can see a differential nuclear cross section for the $\text{PbPb} \rightarrow \text{PbPb} \gamma\gamma$ reaction in heavy-ion UPC at $\sqrt{s_{NN}} = 5.5$ TeV with an extra cut on $W_{\gamma\gamma} > 5.5$ GeV as a function of diphoton invariant mass ($W_{\gamma\gamma} = M_{\gamma\gamma}$). Results are presented for the monopole form factor (this comes from the Yukawa density) — black/blue lines, and for realistic charge distribution — grey/red lines. Contribution of boxes (dashed lines) and results for the VMD-Regge mechanism (solid lines) are collected. The cross section obtained with the monopole form factor is more than 10% bigger than that obtained with the form factor which is calculated as a Fourier transform of the charge distribution in the nucleus. The difference between the two results becomes larger with larger value of the diphoton energy. The competition of the two mechanisms seems to be interesting. While at low

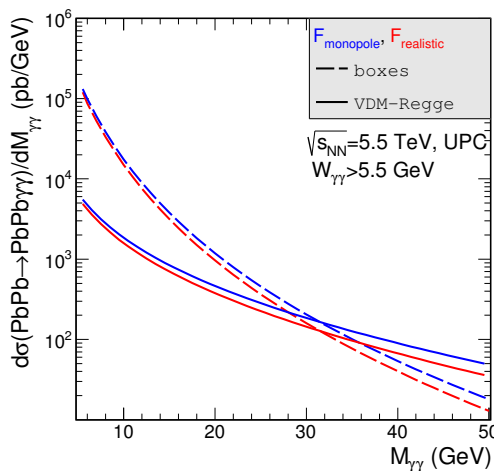


Fig. 2. (Color online) Differential cross section for the light-by-light scattering in lead–lead UPC at $\sqrt{s_{NN}} = 5.5$ TeV with extra cut on $W_{\gamma\gamma} > 5.5$ GeV.

energies, the box contribution wins, at $M_{\gamma\gamma} > 30$ GeV, the VDM-Regge contribution is bigger. The importance of VDM-Regge component is correlated with value of $p_{t,\gamma}$ that is taken into account in nuclear calculation. For presented profile in Fig. 2, the total nuclear cross section for boxes is about one order of magnitude larger comparing to the result for soft VDM-Regge mechanism. However, putting a cut on $p_{t,\gamma} > 2$ GeV, the mentioned difference is about ten orders of magnitude. Detailed set of the cross sections for different limitation on single photon energy or rapidity can be found in Ref. [18].

Two years ago, ATLAS measured a fiducial cross section of $\sigma = 70 \pm 24(\text{stat.}) \pm 17(\text{syst.})$ nb [16] and our theoretical calculations (including experimental acceptance) gave 49 ± 10 nb [18]. The ATLAS comparison of its experimental results to the predictions from Ref. [18] shows a reasonable agreement (see Fig. 3 in Ref. [16]). Only 13 events were observed by the ATLAS Collaboration. This detector recorded data using $480 \mu\text{b}^{-1}$ of lead–lead collision at the centre-of-mass energy per nucleon pair of 5.02 TeV. The measurement of diphoton pair was done in the midrapidity region. The $\gamma\gamma$ invariant mass was limited to $M_{\gamma\gamma} > 6$ GeV. Very recently, the ATLAS Collaboration presented a new result corresponding to an integrated luminosity of 1.73 nb^{-1} , collected in November 2018 [19]. Counting 59 events, they got the fiducial cross section equal to $78 \pm 13(\text{stat.}) \pm 7(\text{syst.}) \pm 3(\text{lumi.})$ nb. Simultaneously, they obtained the experiment-to-theory ratio on the level of 1.59 ± 0.33 . We can expect some additional process that gives two-photon state in the final channel. Analysis of high-energy (2-gluon exchange) processes seems to be crucial in this context.

Similarly as the ATLAS Collaboration, the CMS group measured the same process but for somewhat lower threshold of invariant mass of the produced diphotons [17]. The measured fiducial LbL scattering cross section equals $120 \pm 46(\text{stat.}) \pm 28(\text{syst.}) \pm 4(\text{theo.})$ nb. Using our EPA in the impact parameter space and including realistic form factor, we obtain a value (103 ± 0.034) nb which is in good agreement with the CMS result. Figure 3 shows the CMS preliminary experimental data (light grey/red points) together with our theoretical results (dark grey/blue area). Panel (a) illustrates diphoton invariant mass distribution and panel (b) corresponds to rapidity distribution of single outgoing photon. One can observe rather large statistical uncertainties. Our calculations agree with the data but it seems to be important to further test the LbL scattering with a better precision.

Our approach focusses on the consideration of nucleus as an object with realistic charge distribution. Our numerical results contain a small margin of error (on the level of $< 1\% \times \sigma_{AA \rightarrow AA\gamma\gamma}$) that comes from numerical precision. We do not include the error originating from the monopole or point-like form factor.

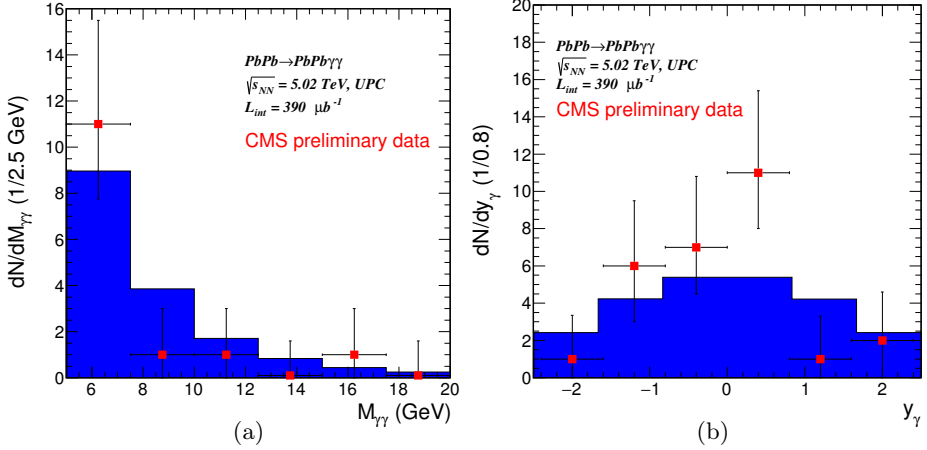


Fig. 3. Comparison of our results (dark grey/blue histogram) with existing CMS preliminary data (light grey/red points) [17]. (a) Invariant mass of diphoton pair. (b) Rapidity of single outgoing photon.

Due to relatively large cuts on the photon transverse momenta, only relatively large diphoton invariant masses were measured by the ATLAS and CMS collaborations. We believe that in a future, one could go to larger luminosity, higher collision energies, better statistics and smaller diphoton invariant masses. In a spirit of future experimental possibilities, predictions for smaller diphoton masses for the midrapidity and more forward region will be presented. The ALICE experiment could measure diphoton state in Pb–Pb UPC at the pseudorapidity range: $-0.9 < \eta_\gamma < 0.9$ and $E_\gamma > 200$ MeV [20]. In this study, we assume that any photon in the pseudorapidity range $2.0 < \eta_\gamma < 4.5$ and with the transverse energy $E_{t,\gamma} > 200$ MeV will be detected by the LHCb [21]. Simultaneously, we know that experimentally some smearing of back-to-back events occurs. We ensure this by application of the experimental energy resolution [22]. Then the transverse momenta of each of the photons takes the form: $p_{i,t} = p_t + \left(\frac{p_t}{E_i}\right) \delta E_i$.

In Table I, one can find values of the total nuclear cross section for fermionic boxes, pionic background and five mesons. Cross section is given in two ranges of the diphoton invariant masses. The first one is from 0 to 2 GeV and the second one from 2 GeV to 50 GeV. Here, a cut on pseudorapidity and energy or transverse momentum of photons is included which corresponds to the ALICE and LHCb conditions. The largest cross-section peaks show up for the $\gamma\gamma \rightarrow \eta \rightarrow \gamma\gamma$ resonance scattering. Additionally, in the range of diphoton invariant mass $M_{\gamma\gamma} > 2$ GeV, comparison of cross sections for fermionic boxes and pionic background clearly shows almost

four-fold dominance of boxes over the unwanted background. Our preliminary predictions suggest that one could be able to measure the QED fermionic signal above $M_{\gamma\gamma} > 2$ GeV.

TABLE I

Total nuclear cross section in nb for the Pb–Pb collision energy 5.02 TeV.

Energy	$W_{\gamma\gamma} = (0-2)$ GeV		$W_{\gamma\gamma} > 2$ GeV	
	ALICE	LHCb	ALICE	LHCb
Fiducial region				
boxes	4 890	3 818	146	79
$\pi^0\pi^0$ background	135 300	40 866	46	24
η	722 573	568 499		
$\eta'(958)$	54 241	40 482		
$\eta_c(1S)$			9	5
$\chi_{c0}(1P)$			4	2
$\eta_c(2S)$			2	1

Figure 4 corresponds to the one of the next runs at the LHC. The energy (per nucleon) of heavy-ion collision was calculated according to the relation: $\sqrt{s_{NN}} = \sqrt{\frac{Z_1 Z_2}{A_1 A_2}} \sqrt{s_{pp}}$ for the future energy in the center-of-mass of proton–proton collision $\sqrt{s_{pp}} = 14$ TeV. Then predicted value for $^{208}\text{Pb}^{82+} - ^{208}\text{Pb}^{82+}$ collision is $\sqrt{s_{NN}} = 5.52$ TeV (Fig. 4 (a)) and for $^{40}\text{Ar}^{18+} - ^{40}\text{Ar}^{18+}$, it is $\sqrt{s_{NN}} = 6.3$ TeV (Fig. 4 (b)). The analysis focusses on lower diphoton invariant masses. At lower diphoton energies ($W_{\gamma\gamma} < 4$ GeV), meson resonances may play an important role in addition to the Standard Model box diagrams or the proposed pionic background. The background is composed of events where exactly two of four outgoing photons are detected. The first one comes from the first pion, and the second one comes from the second pion. The two other photons, from the $\pi^0\pi^0 \rightarrow (\gamma\gamma)(\gamma\gamma)$ decays, are then assumed to be outside of detection area. The inclusion of energy resolution has a significance mainly at $\gamma\gamma \rightarrow \eta, \eta' \rightarrow \gamma\gamma$ resonance scattering and this contribution will be measured with a good statistics. However, the resonance signal is modified including experimental energy resolution [23] and the η and $\eta'(958)$ peaks are about one order of magnitude smaller than without experimental resolution but the total cross section is, of course, still the same. It seems worth mentioning that the peak corresponding to a resonance very strongly depends on the number of bins. These figures suggest that one could be able to measure the “clean” signal above $W_{\gamma\gamma} > 2$ GeV. Comparing Fig. 4 (a) with (b), one can observe that the relevant distribution varies more than two orders of magnitude. In the case of argon–argon collisions, although the collision energy is larger, the predicted cross section

is smaller. This is caused by the fourth power of the charge number of the nucleus in the cross-section formula. The photon flux depends on Z_A^2 so the cross section is multiplied by Z_A^4 . Thus, the total cross section for lead–lead collision is more than two orders of magnitude larger than for the argon–argon collision. However, assuming integrated luminosities of $3.0\text{--}8.8\text{ pb}^{-1}$ in a dedicated Ar–Ar run, obtained cross section allows to get $1460\text{--}4280$ signal events [24].

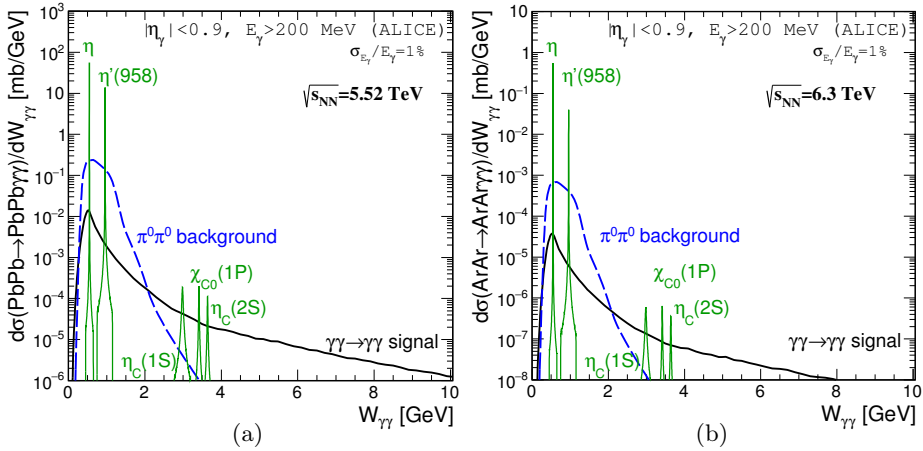


Fig. 4. Differential cross section as a function of $W_{\gamma\gamma} = M_{\gamma\gamma}$ for (a) $\text{PbPb} \rightarrow \text{PbPb} \gamma\gamma$ and (b) $\text{ArAr} \rightarrow \text{ArAr} \gamma\gamma$ reaction. Here, the collision energy at the center-of-mass of the heavy-ion collision is 5.52 TeV and 6.3 TeV for lead–lead and argon–argon, respectively.

4. Conclusion

The ultra-peripheral heavy-ion collisions gave a possibility to measure, for the first time, the $\gamma\gamma \rightarrow \gamma\gamma$ scattering. So far, the ATLAS and CMS collaborations measured the LbL scattering for diphoton collision energies $W_{\gamma\gamma} > 6\text{ GeV}$ (ATLAS) and $W_{\gamma\gamma} > 5\text{ GeV}$ (CMS). Calculated by us the Standard Model predictions are roughly consistent with the experimental data. Our results include realistic photon flux that is a Fourier transform of the charge distribution in the nucleus. We have proposed several additional mechanisms that contribute to the two-photon state. Each of them plays an important role at different ranges of diphoton invariant mass or transverse momentum of single photon. Next, we have studied a background from two-pion decay into pairs of measured photons. Here, the condition is that only two out of four photons in the final state are detected. This contribution could be wrongly interpreted as an enhanced $\gamma\gamma \rightarrow \gamma\gamma$ scattering at low energies ($M_{\gamma\gamma} < 2\text{ GeV}$). The signal-to-background ratio will be improved by including an extra cut *i.e.* on scalar/vector asymmetry or transverse

momentum of the $\gamma\gamma$ pair [22]. The $\gamma\gamma$ scattering through pseudoscalar and scalar mesons have been studied too. The $\gamma\gamma \rightarrow \eta, \eta' \rightarrow \gamma\gamma$ resonance scattering could be measured with good statistics. Comparing contributions for lead–lead and argon–argon collisions, one can conclude that collision of lighter nuclei is less favourable as far as the cross section is considered but one could expect a rather large value of luminosity that will give very satisfactory number of events.

This work has been supported by the National Science Centre, Poland (NCN) grant DEC2014/15/B/ST2/02528.

REFERENCES

- [1] H. Euler, B. Kockel, *Naturwissenschaften* **23**, 246 (1935).
- [2] W. Heisenberg, H. Euler, *Z. Physik* **98**, 714 (1936).
- [3] A. Akhieser, L. Landau, I. Pomeranchuk, *Nature* **138**, 206 (1936).
- [4] T. Hahn, M. Pérez-Victoria, *Comput. Phys. Commun.* **118**, 153 (1999).
- [5] G.J. van Oldenborgh, J.A.M. Vermaseren, *Z. Phys. C* **46**, 425 (1990).
- [6] M. Kłusek-Gawenda, W. Schäfer, A. Szczurek, *Phys. Lett. B* **761**, 399 (2016).
- [7] P. Lebiedowicz, A. Szczurek, *Phys. Lett. B* **772**, 330 (2017).
- [8] C. Patrignani *et al.* [Particle Data Group], *Chin. Phys. C* **40**, 100001 (2016).
- [9] M. Kłusek-Gawenda, A. Szczurek, *Phys. Rev. C* **87**, 054908 (2013).
- [10] S. Uehara *et al.* [Belle Collaboration], *Phys. Rev. D* **79**, 052009 (2009).
- [11] H. Marsiske *et al.* [Crystal Ball Collaboration], *Phys. Rev. D* **41**, 3324 (1990).
- [12] E. Fermi, *Nuovo Cim.* **2**, 143 (1925).
- [13] C.F. Weizsäcker, *Z. Phys.* **88**, 612 (1934).
- [14] E.J. Williams, *Phys. Rev.* **45**, 729 (1934).
- [15] G.P. Lepage, *J. Comput. Phys.* **27**, 192 (1978).
- [16] M. Aaboud *et al.* [ATLAS Collaboration], *Nature Phys.* **13**, 852 (2017).
- [17] A.M. Sirunyan *et al.* [CMS Collaboration], [arXiv:1810.04602](https://arxiv.org/abs/1810.04602) [hep-ex].
- [18] M. Kłusek-Gawenda, P. Lebiedowicz, A. Szczurek, *Phys. Rev. C* **93**, 044907 (2016).
- [19] ATLAS Collaboration, ATLAS-CONF-2019-002.
- [20] B.B. Abelev *et al.* [ALICE Collaboration], *Int. J. Mod. Phys. A* **29**, 1430044 (2014).
- [21] M. Clemencic *et al.* [LHCb Collaboration], *J. Phys.: Conf. Ser.* **331**, 032023 (2011).
- [22] M. Kłusek-Gawenda, *EPJ Web Conf.* **199**, 05004 (2019) [[arXiv:1809.03823](https://arxiv.org/abs/1809.03823) [hep-ph]].
- [23] S. Acharya *et al.* [ALICE Collaboration], *Eur. Phys. J. C* **78**, 263 (2018).
- [24] Z. Citron *et al.*, [arXiv:1812.06772](https://arxiv.org/abs/1812.06772) [hep-ph].